Electronic Supplementary Information for:

Overcoming interpenetration in ladder frameworks using a large readily accessible aliphatic linker

Table of Contents

CCDC search details

A search of the Cambridge Structural Database (CSD) was performed using ConQuest (Cambridge Crystallographic Data Centre). The search was designed to identify MOFs containing ligands with fused benzene rings arranged in a 1,4-linked (para-connected) fashion. Substructure queries were constructed to capture extended aromatic systems comprising consecutively fused phenylene units. Appropriate constraints were applied to ensure connectivity consistent with 1,4-linkage between rings. The search was performed using the most recent version of the CSD available at the time of analysis. No reported MOF structures were identified that incorporate ligands containing more than three consecutively fused 1,4-linked benzene rings, indicating that the ligand architecture presented in this work extends beyond those currently represented in the database.

Figure S1. Annotated ligand **L**, marking the atoms used to measure length (blue), the imide rings used to calculate metal binding angle (red), and the atoms used to measure polynorbornane torsion (yellow).

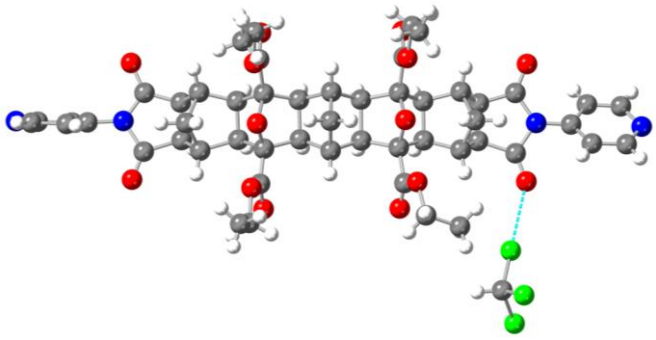

Figure S2. Halogen bond between **L2** and bound chloroform in $[Zn_2\mathbf{L}_3(NO_3)_4]\cdot CHCl_3$. Chloroform forms a halogen bond with the imide carbonyl of **L2**, this bond is 2.890(9) Å (shorter than the sum of van der Waals radii of 3.27 Å) and 4.50° from co-linearity with the C-Cl bond.

Table S1. Spatial data for bis(4-pyridyl) ligand **L** in varying environments.

	Free	$[Zn_2\mathbf{L}_3(NO_3)_4]$		
Ligand		L1	L2	L3
Length (Å)[a]	24.700(7)	24.42(1)	24.28(1)	24.70(1)
Angle (N-N)°)[b]	174	175	173	170
Torsion (°)[c]	1.20(9)	1.8(7)	2.9(7)	0.3(7)

[a]Measured from the pyridyl nitrogen N-N distance. [b]Measured from the planes of the imide rings. [c]Measured from the terminal norbornane carbons.

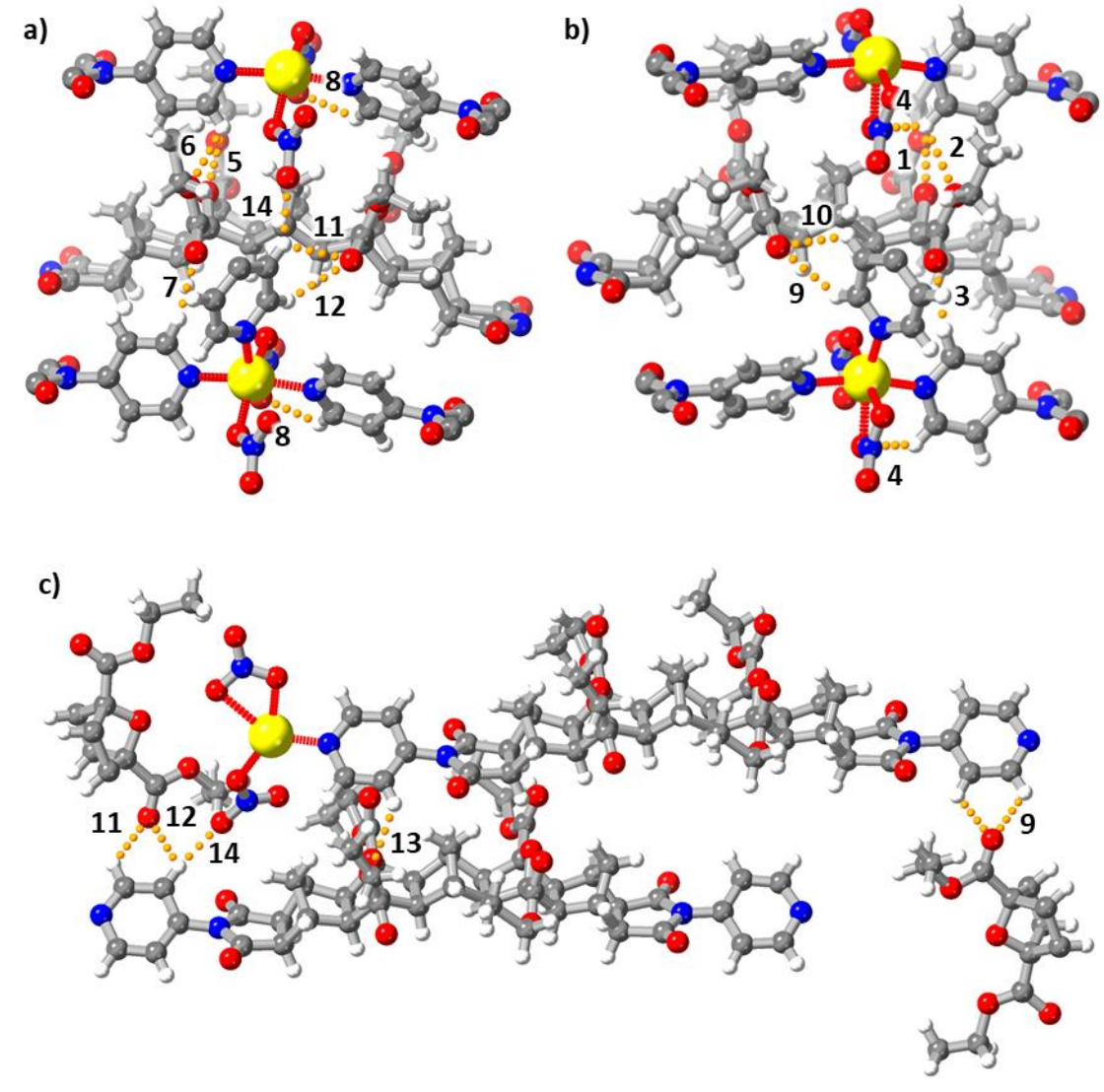

.

Figure S3. Pyridyl C−H···O interactions in (a) **L1** (b) **L2** and (c) **L3** in the structure of $[Zn_2\mathbf{L}_3(NO_3)_4]\cdot CHCl_3$.

Table S2. Pyridyl C−H···O interactions in $[Zn_2\mathbf{L}_3(NO_3)_4]\cdot CHCl_3$, labels refer **Figure S3**.

Label	Donor	Acceptor	C−H···O Distance (Å)	∠C−H···O (°)	Energy (kCalmol^{-1})	Energy (kCalmol^{-1})
1	L1(Ortho)	L1 (Oxanorbornane)	3.29(1)	131	0.53	2.2
2	L1(Ortho)	L1 (Ethoxy)	3.14(1)	109	0.17	0.71
3	L1(Ortho)	L1 (Ester Carbonyl)	3.21(1)	163	2.51	10.5
4	L1(Ortho)	NO_3 (Zn1)	3.02(1)	116	1.47	6.15
5	L2(Ortho)	L2 (Ethoxy)	3.23(1)	132	0.70	2.9
6	L2(Ortho)	L2 (Oxanorbornane)	3.13(1)	109	0.18	0.75
7	L2(Ortho)	L2 (Ester Carbonyl)	3.23(1)	160	2.45	10.25
8	L2(Ortho)	NO_3 (Zn2)	3.14(1)	130	1.33	5.56
9	L3(Ortho)	L1 (Ester Carbonyl)	3.07(1)	117	0.49	2.05
10	L3(Meta)	L1 (Ester Carbonyl)	3.03(1)	117	0.14	0.59
11	L3(Ortho)	L2 (Ester Carbonyl)	3.16(1)	122	0.55	2.3
12	L3(Meta)	L2 (Ester Carbonyl)	3.14(1)	116	0.07	0.3
13	L3(Meta)	L3 (Ester Ethoxy)	3.43(1)	137	0.57	2.4
14	L3	NO_3 (Zn2)	3.17(1)	147	1.74	7.28

General Experimental

Chemicals were purchased from Sigma-Aldrich with the exception of norbornene exo-anhydride **8** (Combi-Blocks) and 2,5-norbornadiene **5** (AK Scientific). All chemicals were used as received with the exception of anhydrous *tert*-butyl hydroperoxide (*t*-BuOOH), which was prepared in toluene according to the method described by Sharpless.[3] The $RuH_2(CO)(PPh_3)_3$ catalyst was prepared according to the method described by Ahmed *et al.*[4] Tetrahydrofuran (THF) was dried by passage through a silica gel 60 (230–400 mesh) column and stored over 4 Å molecular sieves.[5]

^{1}H NMR and ^{13}C NMR were recorded on a Bruker Ascend 400 or 500 MHz FT-NMR spectrometer. HRMS data was recorded using a Shimadzu LCMS-9030 QTOF mass spectrometer. FT-IR data for $[Zn_2\mathbf{L}_3(NO_3)_4]$ was recorded using a Bruker Alpha FT-IR spectrometer and for **L** using a Cary 630 FTIR ATR spectrophotometer with a single-bounce diamond ATR accessory over the range 600–4000 cm^{-1}. Melting points of compounds were determined using a Stuart SMP30 melting point apparatus.

Microwave reactions were performed using a CEM Discover S-Class Explorer 48 Microwave reactor, with continuous irradiation power ranging from 0–300 W as specified and an operational frequency of 50–60 Hz. All reactions were performed in 10 mL vials and sealed with 'snap' caps.

Crystallographic data was collected using the MX1 and MX2 beamlines at the Australian Synchrotron.[6] Crystals were mounted from their respective mother liquors with the assistance of paratone oil before crystallographic data was collected under a stream of nitrogen at 100 K. Crystal structures were solved using the program SHELXT[7] and refined using SHELXL[8] within Olex2 graphic user interface.[9] Coordination geometry and topology were calculated from single crystal structures using SHAPE[1] and ToposPro[2] respectively. Experimental powder diffraction data for $[Zn_2\mathbf{L}_3(NO_3)_4]$ was collected on an XtaLAB Synergy diffractometer employing Cu Kα (λ = 1.5418 Å). Powder diffraction data for $[Zn_2\mathbf{L}_3(NO_3)_4]$ after activation was collected using a STOE STADI P diffractometer operating in the Debye–Scherrer geometry equipped with three Mythen detectors in stationary mode and Mo Kα (0.70930 Å) radiation. Calculated PXRD patterns were generated from single crystal structures and were calculated using Mercury.[10]

Thermal gravimetric analysis (TGA) was conducted using a PerkinElmer TGA 8000 instrument, samples being held in ceramic crucibles under high purity nitrogen.

Elemental analysis data for $[Zn_2\mathbf{L}_3(NO_3)_4]$ was provided by the Elemental Microanalysis Service at Maquarie University.

Gas sorption isotherms were measured by a volumetric method using a Micromeritics 3Flex Surface Characterization Analyser and recorded at low pressures (0 – 1.2 bar); software V6.02. N_2 and H_2 isotherms were measured at 77 K and CO_2 at 273 K and 293 K. For 77 K liquid nitrogen was used. For 273 K and 293 K a Micromeritics ISO-Controller was used for temperature regulation with precision to within 0.01 °C. Gas sorption measurements were performed using ultra-high purity N_2 (≥ 99.999%), H_2 (≥ 99.999%) and CO_2 (≥ 99.995%)

gases. Samples were evacuated and activated on a Smart VacPrep instrument at 120 °C under dynamic vacuum at 10–6 Torr for 24 h to remove residual solvent molecules.

Accessible surface areas and pore size distributions were calculated using Zeo++. The framework structure obtained from single-crystal X-ray diffraction was used as the input. A probe radius of 1.2 Å was employed to determine the accessible surface area and pore characteristics. Pore limiting diameter (PLD) and largest cavity diameter (LCD) were calculated using standard geometric analysis algorithms implemented in the software. All calculations were performed using default grid and sampling parameters unless otherwise stated.

Synthesis

(1α,2β,6β,7α)-4-(pyridine-4-yl)-4-azatricyclo[5.2.1.$0^{2,6}$]dec-8-ene-3,5-dione (3)

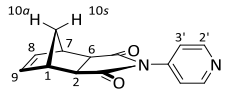

Norbornene-*exo*-anhydride **8** (2.00 g, 12.2 mmol, 1 equiv.) and 4-aminopyridine **9** (1.19 g, 12.7 mmol, 1.04 equiv.) were suspended in DMF (12 mL) in a 25 mL RBF. The flask was then fitted with an air condenser and heated to 130 °C in a sand bath and stirred for 16 hours. During this time, the reagents dissolved to form a brown-tinted solution.

A white powder was then precipitated by the dropwise addition of water before the resultant suspension was poured over cold water (60 mL). The mixture was stirred for 20 minutes before the product was collected using vacuum filtration, washing the solid with water (10 mL) and drying under vacuum to yield imide **3** as a white powder (2.55 g, 10.6 mmol, 87%).

mp: 169.1-169.5 °C. (lit. 158-160 °C)[11]

^{1}H NMR (400 MHz, $CDCl_3$) δ 8.73 (d, *J* = 5.3 Hz, 2H, $H_{2'}$), 7.38 (d, *J* = 5.1 Hz, 2H, $H_{3'}$), 6.37 (s, 2H, $H_{8,9}$), 3.43 (s, 2H, $H_{1,7}$), 2.90 (s, 2H, $H_{2,6}$), 1.64 (d, *J* = 9.9 Hz, 1H, H_{10a}), 1.43 (d, *J* = 9.8 Hz, 1H, H_{10s}).

^{13}C NMR (100 MHz, $CDCl_3$) δ 176.1, 150.8, 139.7, 138.2, 120.1, 48.0, 46.2, 43.2.

HRMS calcd. for $C_{14}H_{12}N_2O_2$ $[M + H]^+$ 241.09715; found 241.10047.

Tetraethyl (1α,2β,5β,6α,7β,10β)-tetracyclo[4.4.1.$0^{2,5}$.$0^{7,10}$]undeca-3,8-diene-3,4,8,9-tetracarboxylate (7)

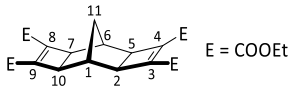

2,5-norbornadiene **5** (2.20 mL, 1.99 g, 21.6 mmol), diethylacetylene dicarboxylate **6** (8.77 mL, 9.36 g, 55.0 mmol, 2.54 equiv.) and $RuH_2(CO)(PPh_3)_3$ (570 mg, 0.621 mmol, 0.29 equiv.) were combined in DMF (6.0 mL). The reaction vessel was equipped with an air condenser before heating to 100 °C for 16 hours and stirred in a sand bath behind a blast shield (caution, exothermic). After cooling on ice, water was added dropwise to the mixture, causing the precipitation of crude product as a dark brown powder which was collected using vacuum filtration.

The resultant dark brown powder was recrystallised from hot EtOH (adding a drop of water while boiling) to produce needle-like brown crystals. The crystals were collected using vacuum filtration, washing with cold MeOH (10 mL) to yield the desired pure product (4.28 g, 46%).

mp: 98.9–99.7 °C.

^{1}H NMR (400 MHz, $CDCl_3$) δ 4.23 (q, *J* = 7.1 Hz, 8H, 4 × Et CH_2), 2.75 (s, 4H, $H_{2,5,7,10}$), 2.41 (s, 2H, $H_{1,6}$), 1.39 (s, 2H, H_{11}), 1.32 (t, *J* = 7.1 Hz, 12H, 4 × Et CH_3).

^{13}C NMR (100 MHz, $CDCl_3$) δ 161.2, 142.5, 61.1, 46.1, 31.8, 23.8, 14.3.

HRMS calcd. for $C_{23}H_{28}O_8$ $[M + Na]^+$ 455.16764; found 455.16976.

Tetraethyl 4,10-dioxahexacyclo [5.5.1.$0^{2,6}$.$0^{3,5}$.$0^{8,12}$.$0^{9,11}$]trideca-3,5,9,11-tetracarboxylate (4)

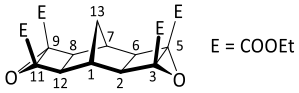

Under an inert N_2 atmosphere, a solution of tetraester **7** (1.00 g, 2.31 mmol) in anhydrous THF (150 mL) was cooled on an ice bath before a solution of *t*-BuOOH in toluene (1.52 mL, 3.824 M, 5.81 mmol, 2.5 equiv.) was added dropwise. The mixture was stirred vigorously for 10 minutes before the addition of *t*-BuOK (140 mg, 1.25 mmol, 0.54 equiv.) in two portions, the second portion being added 30 minutes after the first. The mixture was then stirred for a further 10 minutes before being allowed to warm to room temperature and left to stir for 16 hours. Saturated sodium sulfite was used to quench the reaction, with the biphasic mixture stirred for an additional 20 minutes. The mixture was then reduced to approximately one third of its original volume under reduced pressure and the aqueous phase was extracted with $CHCl_3$ (4 × 60 mL). The organic phases were then combined and dried ($MgSO_4$) and the solvent was removed under reduced pressure. The resultant yellow-tinged liquid solidified upon standing at room temperature in air. The solid was then triturated (*i*-PrOH). Collection using vacuum filtration and washing with *i*-PrOH (10 mL) yielded the pure product as a white powder (461 mg, 43%).

mp: 121.4–123.8 °C.

^{1}H NMR (400 MHz, $CDCl_3$) δ 4.27 (ABX_3, J_{AB} = 10.8 Hz, J_{AX} = J_{BX} = 7.1 Hz, 8H, 4 × Et CH_2), 3.29 (s, 2H, $H_{1,7}$), 2.26 (s, 4H, $H_{2,6,8,12}$), 1.94 (s, 2H, H_{11}), 1.31 (t, *J* = 7.1 Hz, 12H, 4 × Et CH_3).

^{13}C NMR (100 MHz, $CDCl_3$) δ 163.9, 64.4, 62.1, 48.9, 36.7, 28.7, 14.3.

HRMS calcd. For $C_{23}H_{28}O_{10}$ $[M + Na]^+$ 487.15745; found 487.15987.

Tetraethyl (1α,2β,3α,4β,5α,6β,10β,11α,12β,13α,14β,15α,16β,17α,18β,19α,20β,24β,25α,26β,27α,28β)-7,9,21,23-tetraoxo-8,22-*bis*(pyridine-4-yl)-30,32-dioxa-8,22-diazadodecacyclo[13.13.1^{1,15}.1^{3,13}.1^{5,11}.1^{17,27}.1^{19,25}.0^{2,14}.0^{4,12}.0^{6,10}.0^{16,28}.0^{18,26}.0^{20,24}]tritriaconta-3,13,17,27-tetracarboxylate (Ligand L)

The *bis*-epoxide **4** (261 mg, 0.56 mmol) and pyridine imide **3** (284 mg, 1.18 mmol, 2.1 equiv.) were combined in DMF (2.0 mL) in a 10mL microwave vial before being heated to 140 °C for 30 minutes with microwave radiation (200W). The mixture was allowed to cool before water was added to precipitate an off-white powder. The crude solid was collected using vacuum filtration and washed with *i*-PrOH, drying under vacuum to yield the final product as a white powder (427 mg, 80%).

mp: > 330°C dec.

FT-IR (ATR, cm^{-1}): 2970 (w), 1720 (s), 1590 (w), 1380 (m), 1300 (m), 1180 (m), 1090 (s), 802 (m), 690 (m).

^{1}H NMR (500 MHz, $CDCl_3$) δ 8.63 (dd, *J* = 1.9 Hz, *J* = 4.9 Hz, 2H, $H_{6'}$), 7.85 (td, *J*′ = 7.8 Hz, *J* = 1.9 Hz, 2H, $H_{4'}$), 7.36 (dd, *J* = 7.6 Hz, *J* = 4.8 Hz, 2H, $H_{5'}$), 7.21 (d, *J* = 8.0 Hz, 1H, $H_{3'}$), 4.32 (ABX_3, J_{AB} = 10.9 Hz, J_{AX} = J_{BX} = 7.1 Hz, 8H, 4 × Et CH_2), 2.73 (s, 4H, $H_{6,10,20,24}$), 2.72 (s, 4H, $H_{5,11,19,25}$), 2.40 (d, *J* = 11.8 Hz, 2H, $H_{31a,33a}$), 2.21 (s, 4H, $H_{4,12,18,26}$), 2.10 (s, 2H, $H_{1,15}$), 2.00 (s, 4H, $H_{2,14,16,28}$), 1.92 (s, 2H, H_{29}), 1.33 (t, *J* = 7.1 Hz, 12H, 4 × Et CH_3), 1.06 (d, *J* = 11.8 Hz, 2H, $H_{31s,\ 33s}$).

^{13}C NMR (100 MHz, $CDCl_3$) δ 176.3, 168.2, 150.0, 146.0, 138.7, 124.4, 122.2, 89.8, 61.7, 55.0, 54.8, 48.5, 42.2, 40.7, 29.4, 28.9, 14.6.

HRMS calcd. for $C_{51}H_{52}N_4O_{14}$ $[M + H]^+$ 945.35528; found 945.35484.

NMR Spectra of Organic Compounds

(1α,2β,6β,7α)-4-(pyridine-4-yl)-4-azatricyclo[5.2.1.0^{2,6}]dec-8-ene-3,5-dione (3)

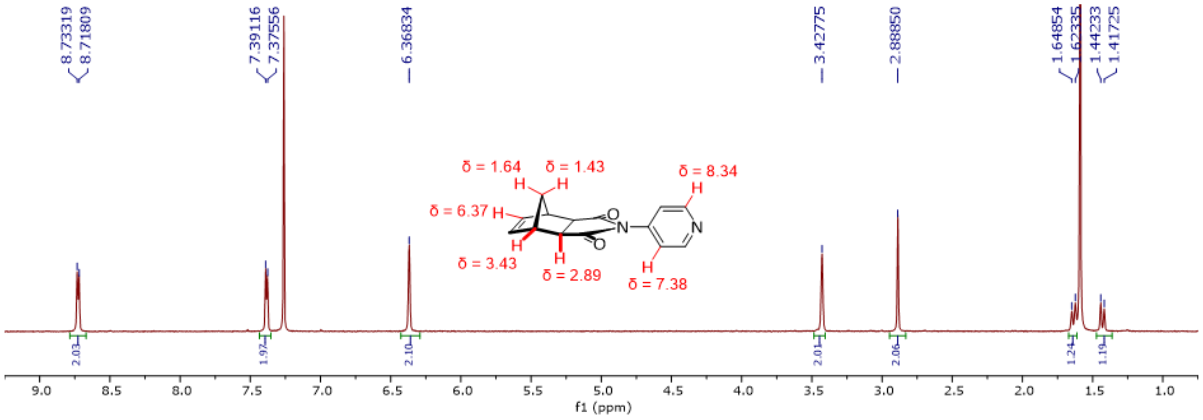

^{1}H NMR (400 MHz, $CDCl_3$) δ 8.73 (d, *J* = 5.3 Hz, 2H, $H_{2'}$), 7.38 (d, *J* = 5.1 Hz, 2H, $H_{3'}$), 6.37 (s, 2H, $H_{8,9}$), 3.43 (s, 2H, $H_{1,7}$), 2.90 (s, 2H, $H_{2,6}$), 1.64 (d, *J* = 9.9 Hz, 1H, H_{10a}), 1.43 (d, *J* = 9.8 Hz, 1H, H_{10s}).

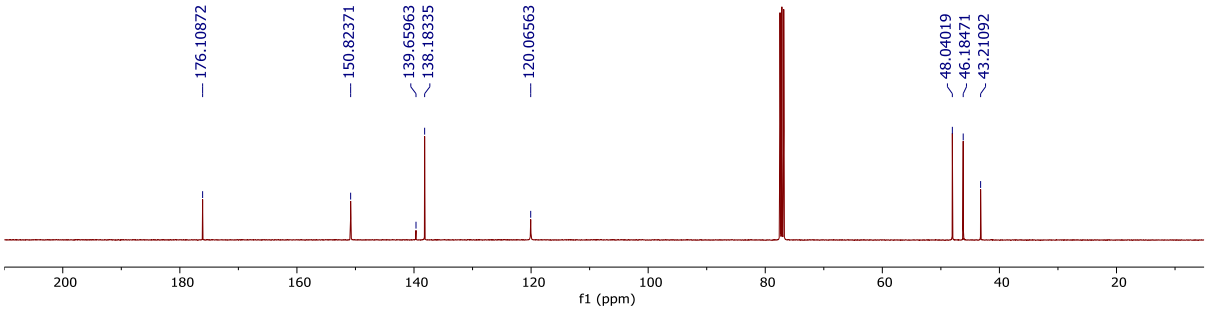

^{13}C NMR (100 MHz, $CDCl_3$) δ 176.1, 150.8, 139.7, 138.2, 120.1, 48.0, 46.2, 43.2.

Tetraethyl (1α,2β,5β,6α,7β,10β)-tetracyclo[4.4.1.0^{2,5}.0^{7,10}]undeca-3,8-diene-3,4,8,9-tetracarboxylate (7)

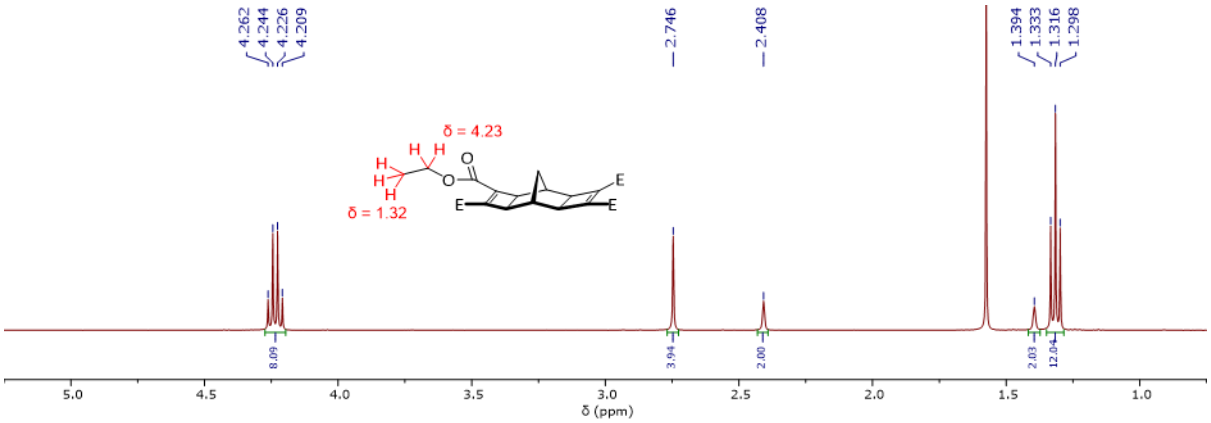

^{1}H NMR (400 MHz, $CDCl_3$) δ 4.23 (q, *J* = 7.1 Hz, 8H, 4 × Et CH_2), 2.75 (s, 4H, $H_{2,5,7,10}$), 2.41 (s, 2H, $H_{1,6}$), 1.39 (s, 2H, H_{11}), 1.32 (t, *J* = 7.1 Hz, 12H, 4 × Et CH_3).

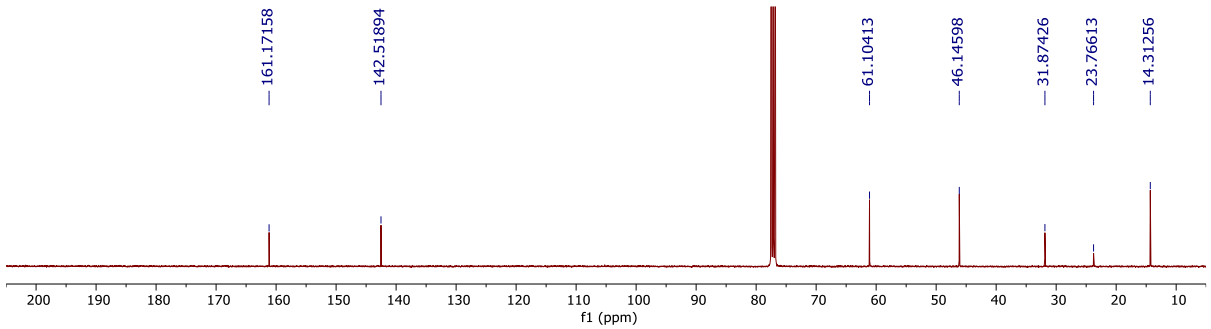

^{13}C NMR (100 MHz, $CDCl_3$) δ 161.2, 142.5, 61.1, 46.1, 31.8, 23.8, 14.3.

Tetraethyl 4,10-dioxahexacyclo [5.5.1.$0^{2,6}$.$0^{3,5}$.$0^{8,12}$.$0^{9,11}$]trideca-3,5,9,11-tetracarboxylate (4)

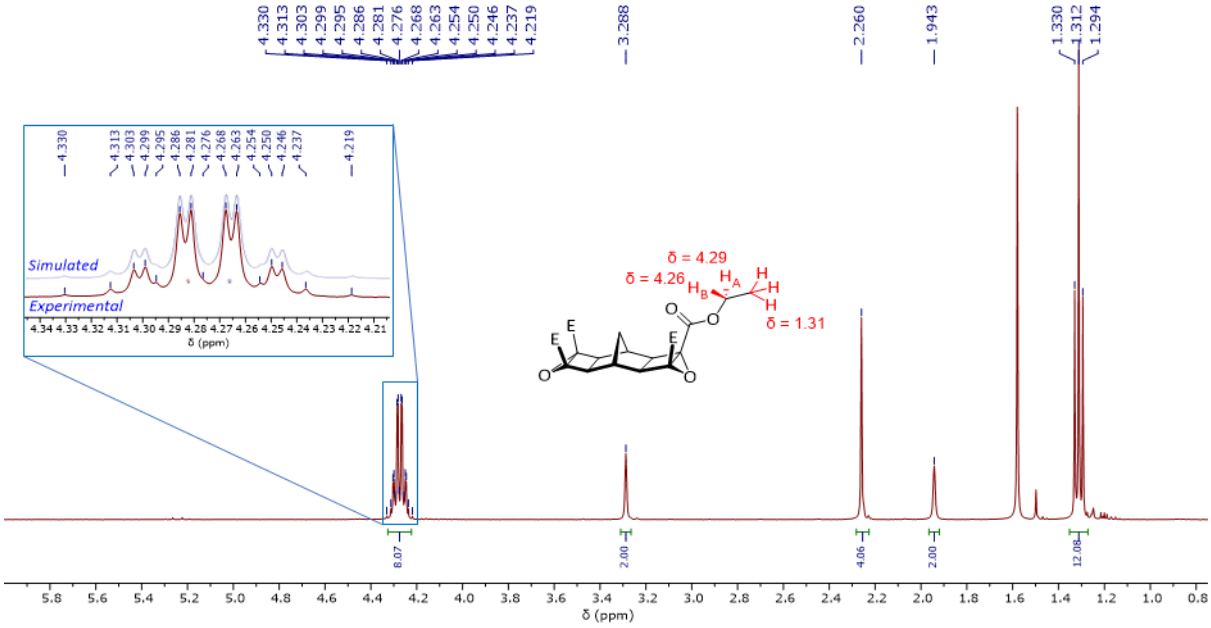

^{1}H NMR (400 MHz, $CDCl_3$) δ 4.27 (ABX_3*, J_{AB} = 10.8 Hz, J_{AX} = J_{BX} = 7.1 Hz, 8H, 4 × Et CH_2), 3.29 (s, 2H, $H_{1,7}$), 2.26 (s, 4H, $H_{2,6,8,12}$), 1.94 (s, 2H, H_{11}), 1.31 (t, J = 7.1 Hz, 12H, 4 × Et CH_3).

*ABX_3 splitting pattern confirmed by simulation (see inset) using WinDNMR[12]

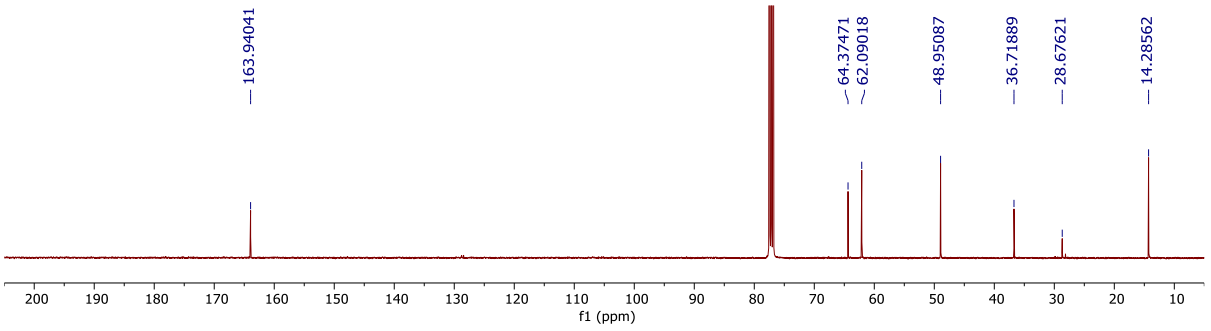

^{13}C NMR (100 MHz, $CDCl_3$) δ 163.9, 64.4, 62.1, 48.9, 36.7, 28.7, 14.3.

Tetraethyl (1α,2β,3α,4β,5α,6β,10β,11α,12β,13α,14β,15α,16β,17α,18β,19α,20β,24β,25α,26β,27α,28β)-7,9,21,23-tetraoxo-8,22-*bis*(pyridine-4-yl)-30,32-dioxa-8,22-diazadodecacyclo[13.13.1^{1,15}.1^{3,13}.1^{5,11}.1^{17,27}.1^{19,25}.0^{2,14}.0^{4,12}.0^{6,10}.0^{16,28}.0^{18,26}.0^{20,24}]tritriaconta-3,13,17,27-tetracarboxylate (L)

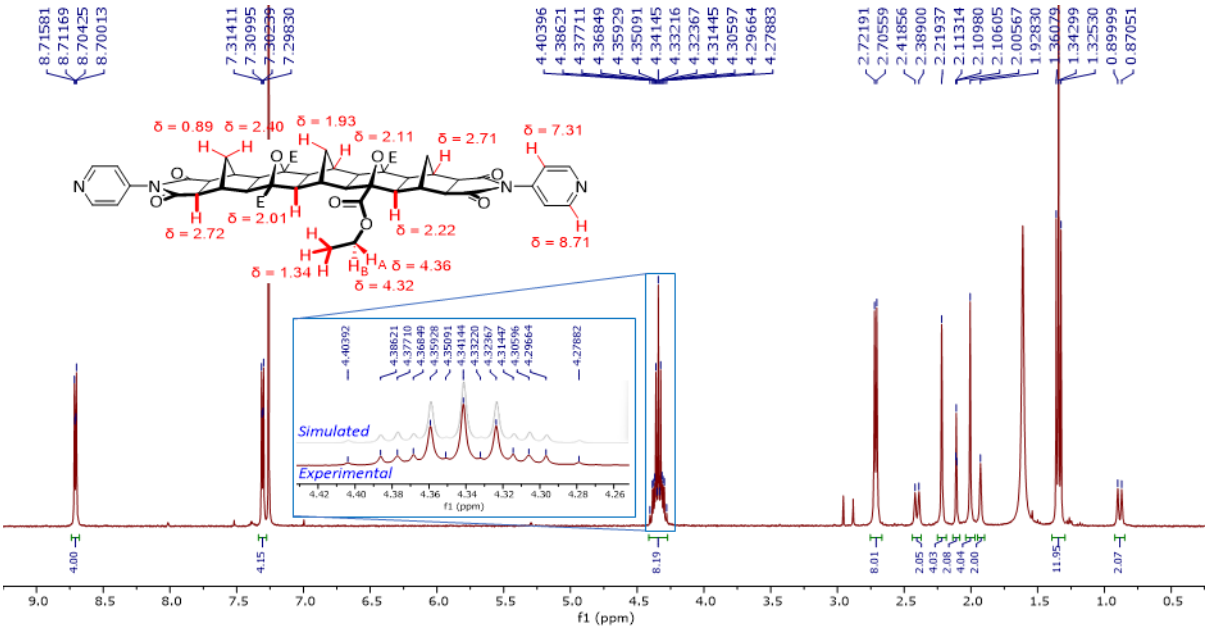

^{1}H NMR (400 MHz, $CDCl_3$) δ 8.71 (app. d, *J* = 6.2 Hz, 4H, $H_{2'}$), 7.31 (app. d, *J* = 6.2 Hz, 4H, $H_{3'}$), 4.34 (ABX$_3$, $J_{AX} = J_{BX}$ = 7.1 Hz, J_{AB} = 10.8 Hz, 8H, 4 × Et CH_2), 2.72 (s, 4H, $H_{6,10,20,24}$), 2.71 (s, 4H, $H_{5,11,19,25}$), 2.40 (d, *J* = 11.8 Hz, 2H, $H_{31a,33a}$), 2.22 (s, 4H, $H_{4,12,18,26}$), 2.11 (s, 2H, $H_{1,15}$), 2.01 (s, 4H, $H_{2,14,16,28}$), 1.93 (s, 2H, H_{29}), 1.34 (t, *J* = 7.1 Hz, 12H, 4 × Et CH_3), 0.89 (d, *J* = 11.8 Hz, 2H, $H_{31s,\ 33s}$).

*ABX$_3$ splitting pattern confirmed by simulation (see inset) using WinDNMR

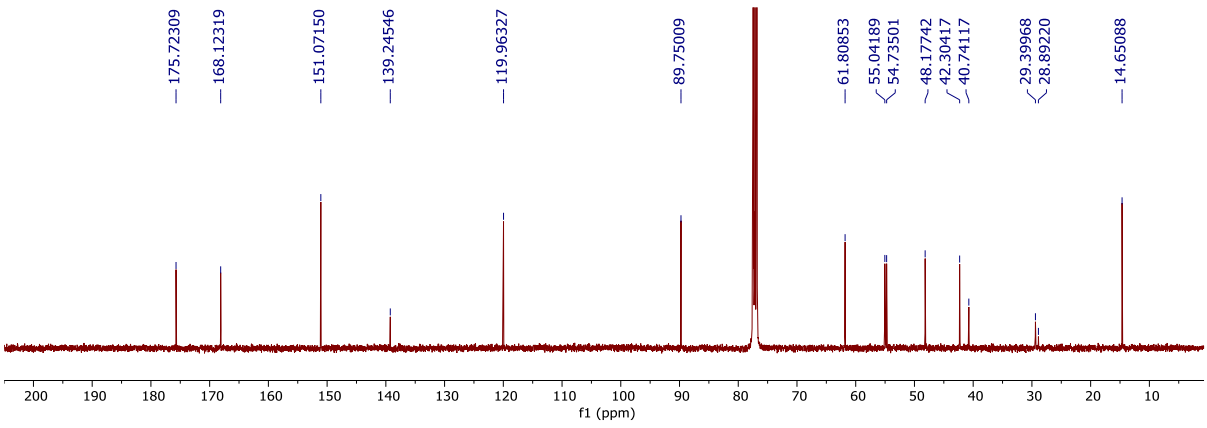

^{13}C NMR (100 MHz, $CDCl_3$) δ 175.7, 168.1, 151.0, 139.2, 120.0, 89.7, 61.8, 55.0, 54.7, 48.2, 42.3, 40.7, 29.4, 28.8, 14.6.

Table S3. Crystallographic parameters of tetraester **7**.

Compound	7
Empirical formula	$C_{23}H_{28}O_8$
Formula weight ($gmol^{-1}$)	432.45
Crystal system	Orthorhombic
Space group	*Pbca*
Temperature (K)	100.0(2)
Crystal size (mm^3)	0.3 × 0.12 × 0.12
Colour	Tan
Habit	Needle
a (Å)	9.842(2)
b (Å)	18.321(4)
c (Å)	23.883(5)
α (°)	90
β (°)	90
γ (°)	90
Volume($Å^3$)	4306.5(15)
Z	8
ρ_{calc} (gcm^{-3})	1.334
μ (mm^{-1})	0.101
F_{000}	1840
Radiation	Synchrotron (λ = 0.710918)
2ϑ range for data collection (°)	3.41 to 58.132
Index ranges	-10 ≤ h ≤ 10, -21 ≤ k ≤ 21, -28 ≤ l ≤ 28
Total/independent reflections	54191/4535 [R_{int} = 0.0320, R_{sigma} = 0.0153]
Data/restraints/parameters	4535/0/124
Goodness-of-fit on F^2	1.07
Final *R* indexes [I>=2σ (I)]	R_1 = 0.0923, wR_2 = 0.2094
Final *R* indexes [all data]	R_1 = 0.0938, wR_2 = 0.2104

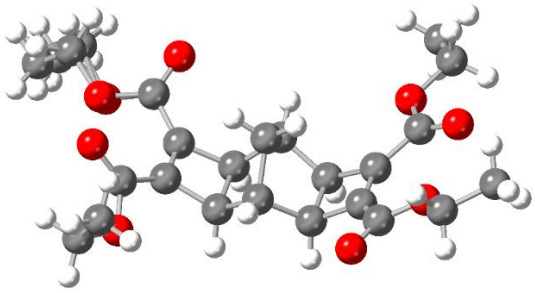

Figure S4. Crystal structure of tetraester **7**.

Table S4. Crystallographic parameters of [*5*]polynorbornane ligand **L**.

Compound	**L**
Empirical formula	$C_{53}H_{57}N_5O_{15}$
Formula weight ($gmol^{-1}$)	1004.03
Crystal system	Monoclinic
Space group	$P2_1/c$
Temperature (K)	100(2)
Crystal size (mm^3)	1.0 × 0.5 × 0.4
Colour	Colourless
Habit	Block
a (Å)	19.067(4)
b (Å)	9.932(2)
c (Å)	27.276(6)
α (°)	90
β (°)	110.27(3)
γ (°)	90
Volume($Å^3$)	4845.3(19)
Z	4
ρ_{calc} (gcm^{-3})	1.376
μ (mm^{-1})	0.102
F_{000}	2120
Radiation	Synchrotron (λ = 0.710759)
2ϑ range for data collection (°)	2.276 to 64.334
Index ranges	-27 ≤ h ≤ 27, -12 ≤ k ≤ 12, -36 ≤ l ≤ 36
Total/independent reflections	82828/14137 [R_{int} = 0.0658, R_{sigma} = 0.0403]
Data/restraints/parameters	14137/0/667
Goodness-of-fit on F^2	1.058
Final *R* indexes [I>=2σ (I)]	R_1 = 0.0682, wR_2 = 0.1914
Final *R* indexes [all data]	R_1 = 0.0706, wR_2 = 0.1968

*Includes contribution of one MeCN and one H_2O

Table S5. Crystallographic parameters of $[Zn_2\mathbf{L}_3(NO_3)_4]\cdot CHCl_3$.

Compound	$[Zn_2\mathbf{L}_3(NO_3)_4]\cdot CHCl_3$
Empirical formula	$C_{154}H_{157}Cl_3N_{16}O_{54}Zn_2$
Formula weight ($gmol^{-1}$)	3333.04
Crystal system	Triclinic
Space group	*P*−1
Temperature (K)	100(2)
Crystal size (mm^3)	0.5 × 0.25 × 0.25
Colour	Colourless
Habit	Needle
a (Å)	10.332(2)
b (Å)	28.578(6)
c (Å)	45.068(9)
α (°)	87.24(3)
β (°)	87.12(3)
γ (°)	89.99(3)
Volume($Å^3$)	13275(5)
Z	2
ρ_{calc} (gcm^{-3})	0.834
μ (mm^{-1})	0.267
F_{000}	3472
Radiation	Synchrotron (λ = 0.71073)
2ϑ range for data collection (°)	0.906 to 57.456
Index ranges	-13 ≤ h ≤ 13, -36 ≤ k ≤ 37, -55 ≤ l ≤ 55
Total/independent reflections	157375/45435 [R_{int} = 0.0670, R_{sigma} = 0.0627]
Data/restraints/parameters	45435/0/744
Goodness-of-fit on F^2	1.508
Final *R* indexes [I>=2σ (I)]	R_1 = 0.1812, wR_2 = 0.4591
Final *R* indexes [all data]	R_1 = 0.2415, wR_2 = 0.5016

*Includes contribution of one $CHCl_3$

The *R* indexes are high due to diffuse scattering and disordered solvent within the large void of the crystal structure. The structure was refined using the solvent mask in Olex2. Such disorder is common for highly porous MOFs.[13]

SHAPE[1] Outputs for $[Zn_2\mathbf{L}_3(NO_3)_4]\cdot CHCl_3$

Zn_1

HP-6 1 D6h Hexagon

PPY-6 2 C5v Pentagonal pyramid

OC-6 3 Oh Octahedron

TPR-6 4 D3h Trigonal prism

JPPY-6 5 C5v Johnson pentagonal pyramid J2

Structure [ML6]	HP-6	PPY-6	OC-6	TPR-6	JPPY-6
Zn1 ,	32.939,	22.870,	3.673,	11.735,	27.673

Zn_2

HP-6 1 D6h Hexagon

PPY-6 2 C5v Pentagonal pyramid

OC-6 3 Oh Octahedron

TPR-6 4 D3h Trigonal prism

JPPY-6 5 C5v Johnson pentagonal pyramid J2

Structure [ML6]	HP-6	PPY-6	OC-6	TPR-6	JPPY-6
Zn2 ,	30.105,	18.596,	6.456,	9.290,	22.212

ToposPro[2] Output for $[Zn_2\mathbf{L}_3(NO_3)_4]\cdot CHCl_3$

Point symbol for net: {4^2.6}c

3-c net; uninodal net

Topological type: (4,4)(0,2) (1D_2D_free.ttd) {4^2.6} - VS [4.4.*] (17944 types in 4 databases)

Elapsed time: 6.02 sec.

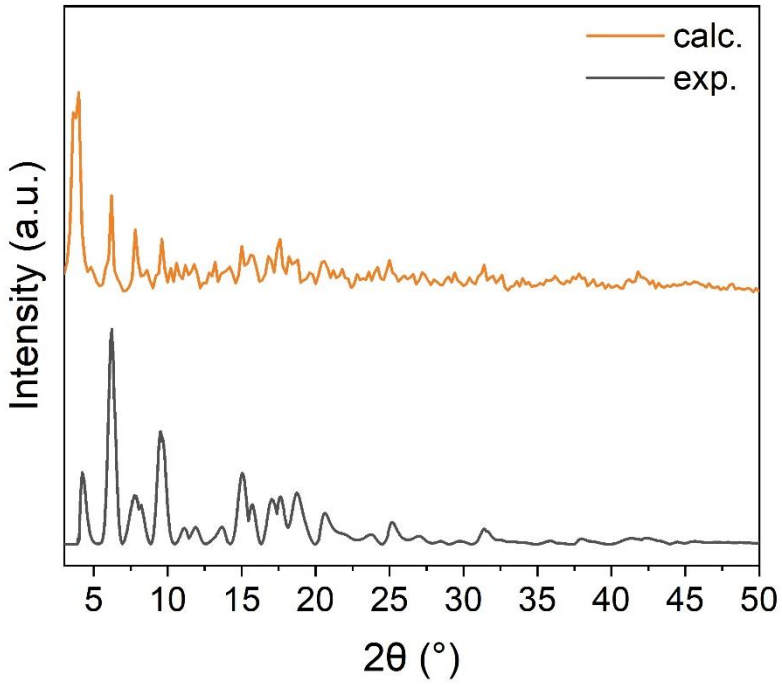

Figure S5. PXRD of $[Zn_2\mathbf{L}_3(NO_3)_4]\cdot CHCl_3$ with calculated (orange) and experimental (black) patterns (Cu Kα (λ = 1.5418 Å).

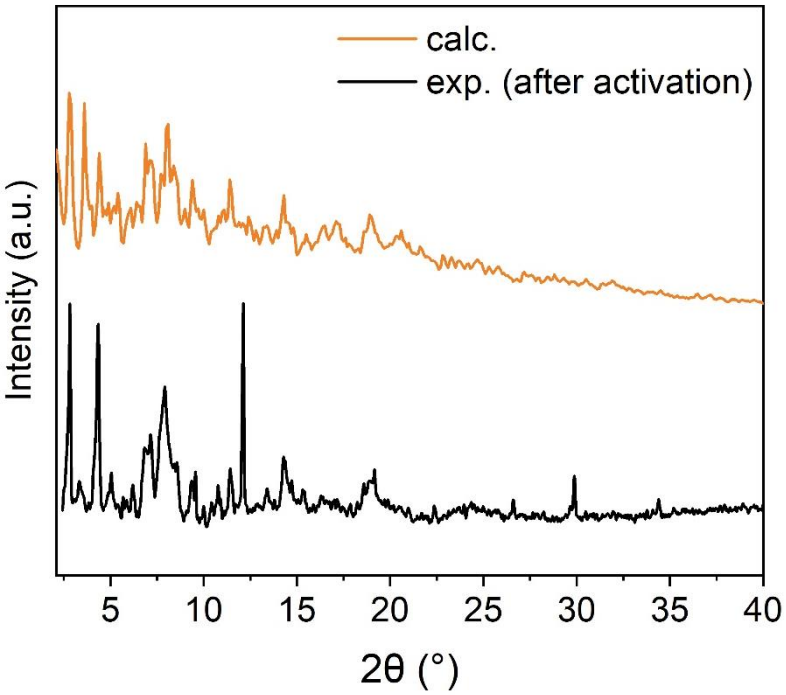

Figure S6. PXRD of activated $[Zn_2\mathbf{L}_3(NO_3)_4]\cdot CHCl_3$ with calculated (orange) and experimental (black) patterns (Mo Kα).

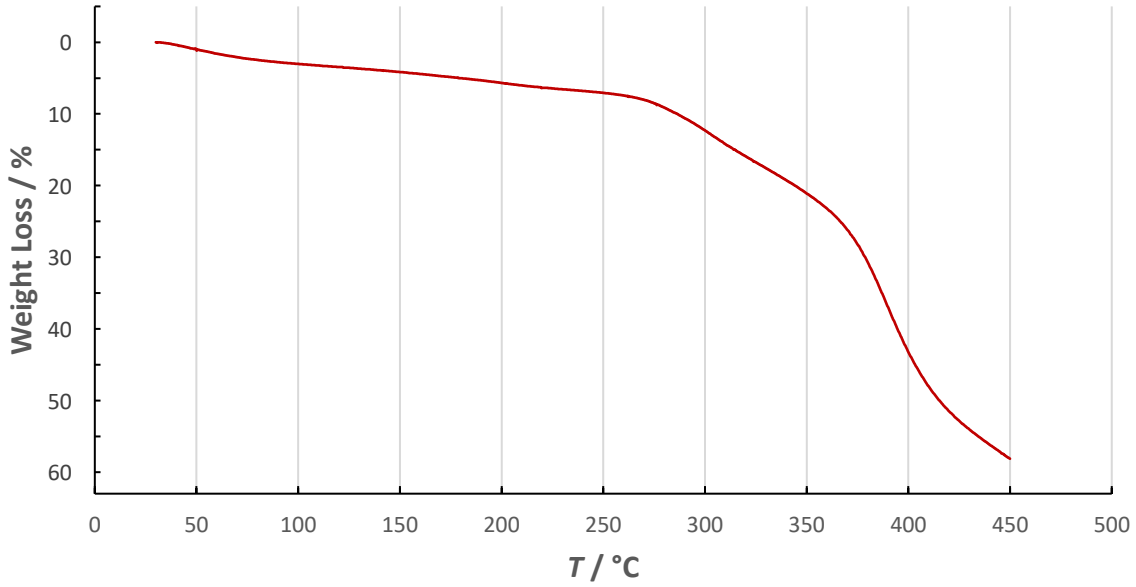

Figure S7. Thermal Gravimetric Analysis (TGA) of $[Zn_2\mathbf{L}_3(NO_3)_4]\cdot CHCl_3$.

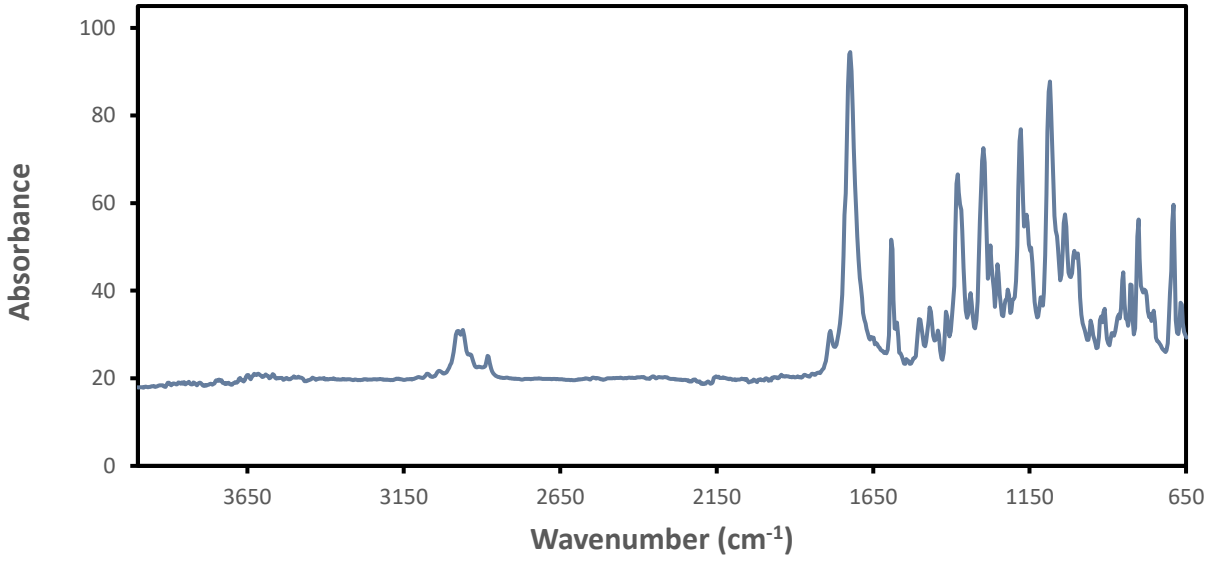

Figure S8. ATR-FTIR spectrum of ligand **L**.

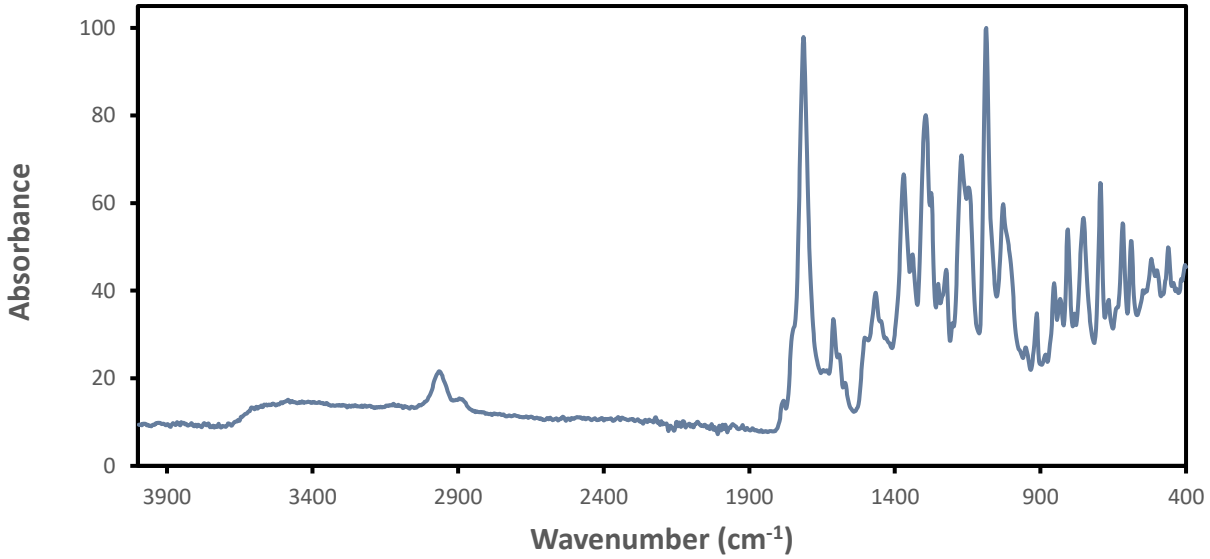

Figure S9. ATR-FTIR spectrum of $[Zn_2\mathbf{L}_3(NO_3)_4]\cdot CHCl_3$.

Gas adsorption measurements

Gas adsorption isotherms of activated $[Zn_2\mathbf{L}_3(NO_3)_4]\cdot CHCl_3$ were recorded at low pressure (0 – 1.2 bar) by a volumetric method using a Micromeritics 3Flex instrument. Approximately 40 mg of dried DCM exchanged sample was weighed in a pre-dried and weighed Quartz BET tube. Using a Micromeritics Smart VacPrep system the sample was evacuated and activated at 80 °C under dynamic vacuum at 10^{-6} Torr for at least 24 h to remove any solvent molecules. An accurate weight of the degassed sample was measured prior to analysis. Gas adsorption measurements were performed using ultra-high purity N_2, H_2 and CO_2 gas received from BOC Gases. When isosteric heats of adsorption isotherms were needed, the gas uptake was measured at two different temperatures.

Calculations of Isoteric heat of adsorption (Q_{st})

The isoteric heat of adsorption (Q_{st}) was calculated from the sorption data measured at 273 K and 293 K. The data were fit to equation 1.

$$\ln \boldsymbol{P} = \ln \boldsymbol{N} + \frac{\mathbf{1}}{\boldsymbol{T}} \sum_{\boldsymbol{i=0}}^{\boldsymbol{m}} \boldsymbol{a_i N^i} + \sum_{\boldsymbol{i=0}}^{\boldsymbol{n}} \boldsymbol{b_i N^i} \qquad \textbf{(1)}$$

To calculate the Q_{st} equation 2 was applied using the fitting parameters from equation 1

$$\boldsymbol{Q_{st}} = -\boldsymbol{R} \sum_{\boldsymbol{i=0}}^{\boldsymbol{m}} \boldsymbol{a_i N^i} \qquad \textbf{(2)}$$

Porosity calculations

Geometric structure analysis of $[Zn_2\mathbf{L}_3(NO_3)_4]\cdot CHCl_3$ was completed using the Zeo++ software suite.[14] The theoretical accessible surface area for N_2 was computed to be 1938.55 $m^2\ cm^{-3}$ with Zeo++.

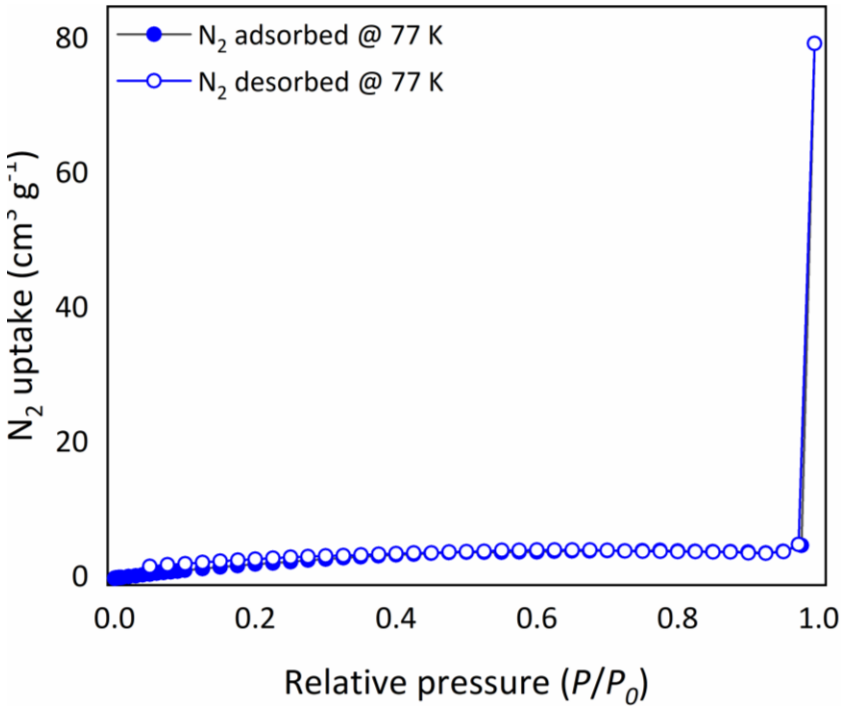

Figure S10. N_2 isotherm of $[Zn_2\mathbf{L}_3(NO_3)_4]\cdot CHCl_3$ at 77 K.

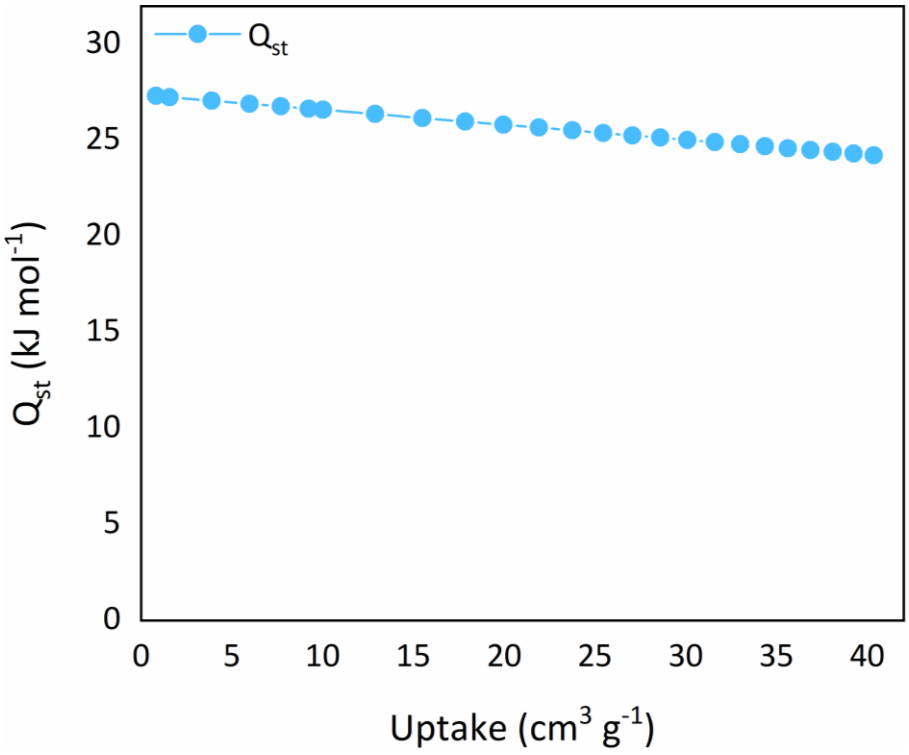

Figure S11. Enthalpy of adsorption (Q_{st}) of $CO2_2$ by $[Zn_2\mathbf{L}_3(NO_3)_4]\cdot CHCl_3$, calculated using the Van't Hoff method.

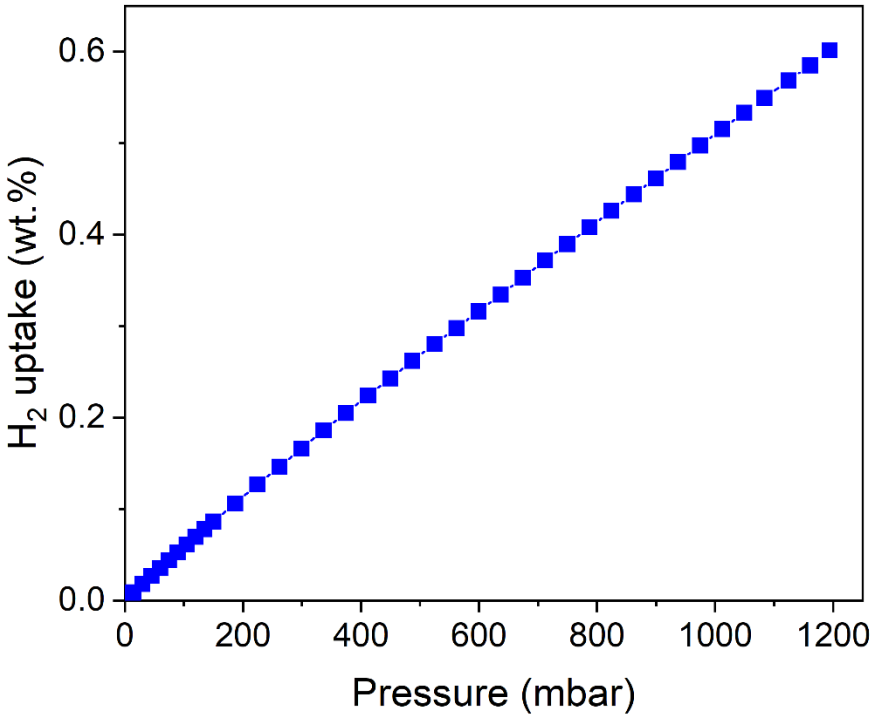

Figure S12. H_2 uptake of of $[Zn_2\mathbf{L}_3(NO_3)_4]\cdot CHCl_3$ as a wt% at 77 K up to 1bar.

References

1. M. Llunell, D. Casanova, J. Cirera, P. Alemany and S. Alvarez, *SHAPE* (Version 2.1), Universitat de Barcelona, Barcelona, Spain, 2013.
2. V. A. Blatov, A. P. Shevchenko and D. M. Proserpio, *Cryst. Growth Des.*, 2014, **14**, 3576-3586.
3. J. G. Hill, B. E. Rossiter and K. B. Sharpless, *J. Org. Chem.*, 2002, **48**, 3607-3608.
4. N. Ahmad, J. J. Levison, S. D. Robinson, M. F. Uttley, E. R. Wonchoba and G. W. Parshall, in *Inorg. Synth.*, ed. G. W. Parshall, McGraw-Hill, United States of America, 1974, vol. 15, ch. Chapter Three Triphenylphosphine Complexes of Transition Metals, pp. 45-64.
5. D. B. Williams and M. Lawton, *J. Org. Chem.*, 2010, **75**, 8351-8354.
6. D. Aragao, J. Aishima, H. Cherukuvada, R. Clarken, M. Clift, N. P. Cowieson, D. J. Ericsson, C. L. Gee, S. Macedo, N. Mudie, S. Panjikar, J. R. Price, A. Riboldi-Tunnicliffe, R. Rostan, R. Williamson and T. T. Caradoc-Davies, *J. Synchrotron Radiat.*, 2018, **25**, 885-891.
7. G. M. Sheldrick, *Acta Crystallogr. A Found. Adv.*, 2015, **71**, 3-8.
8. G. M. Sheldrick, *Acta Crystallogr C Struct. Chem.*, 2015, **71**, 3-8.
9. O. V. Dolomanov, L. J. Bourhis, R. J. Gildea, J. A. K. Howard and H. Puschmann, *J. Appl. Crystallogr.*, 2009, **42**, 339-341.
10. C. F. Macrae, I. Sovago, S. J. Cottrell, P. T. A. Galek, P. McCabe, E. Pidcock, M. Platings, G. P. Shields, J. S. Stevens, M. Towler and P. A. Wood, *J. Appl. Crystallogr.*, 2020, **53**, 226-235.
11. J. V. Hernandez-Madrigal, A. Pineda-Contreras, O. F. Vazquez-Vuelvas, M. A. Tlenkopatchev, H. Garcia-Ortega, R. Gavino-Ramirez and Z. Gomez-Sandoval, *Lett. Org. Chem.*, 2011, **8**, 249-257.
12. H. J. Reich, *J. Chem. Educ.*, 1995, **72**, 1086.
13. S. Øien-Ødegaard, G. C. Shearer, D. S. Wragg and K. P. Lillerud, *Chem. Soc. Rev.*, 2017, **46**, 4867-4876.
14. T. F. Willems, C. H. Rycroft, M. Kazi, J. C. Meza and M. Haranczyk, *Micropor. Mesopor. Mat.*, 2012, **149**, 134-141.